



Evidence for a narrow structure at $W \sim 1.68$ GeV in η photoproduction off the neutron

V. Kuznetsov^{a,b,c,*}, S. Churikova^b, G. Gervino^d, F. Ghio^e, B. Girolami^e, D. Ivanov^b, J. Jang^a, A. Kim^a, W. Kim^a, A. Ni^a, Yu. Vorobiev^b, M. Yurov^a, A. Zabrodin^b

^a *Kyungpook National University, 1370 Sankyuk-dong, Puk-ku, Daegu, Republic of Korea*

^b *Institute for Nuclear Research, 117312 Moscow, Russia*

^c *INFN Laboratori Nazionali del Sud and Università di Catania, 95123 Catania, Italy*

^d *Dipartimento di Fisica Sperimentale, Università di Torino and INFN Sezione di Torino, 10125 Torino, Italy*

^e *INFN Sezione Sanità and Istituto Superiore di Sanità, 00161 Roma, Italy*

Received 7 September 2006; received in revised form 11 January 2007; accepted 15 January 2007

Available online 8 February 2007

Editor: D.F. Geesaman

Abstract

New results on quasi-free η photoproduction on the neutron and proton bound in a deuteron target are presented. The $\gamma n \rightarrow \eta n$ quasi-free cross section reveals a bump-like structure which is not seen in the cross section on the proton. This structure may signal the existence of a relatively narrow ($M \sim 1.68$ GeV, $\Gamma \lesssim 30$ MeV) baryon state.

© 2007 Elsevier B.V. Open access under [CC BY license](http://creativecommons.org/licenses/by/3.0/).

Despite the availability of modern precise experimental data, the complete spectrum of baryons is not yet well established. Among 43 nucleon and delta resonances predicted by QCD-inspired models, almost half have yet to be experimentally identified (“missing” resonances) [1]. Quantum chromodynamics may also allow for more complicated quark systems containing, for example, an additional quark–antiquark pair $q\bar{q}$ (pentaquarks). The existence (or non-existence) of this type of particles is another challenge for both theory and experiment.

Much of our knowledge on the baryon spectrum was obtained through pion–nucleon scattering and meson photoproduction off the proton. Meson photoproduction off the neutron may offer a unique tool to study certain baryons which have still not been firmly established. Some resonances are predicted to be exclusively photoexcited from neutrons and not from protons [2]. For example, a single-quark transition model [3] suggests only weak photoexcitation of the $D_{15}(1675)$ resonance

from the proton target. On the other hand, photocouplings to the neutron calculated in the framework of this approach are not small.

The possible photoexcitation of a non-strange pentaquark state (if it exists) is of high interest as well. This particle is associated with the second nucleon-like member of an antidecuplet of exotic baryons [4,5]. Evidence for the lightest member of the antidecuplet, the $\Theta^+(1540)$ baryon, is now being widely debated [6]. A benchmark signature of the non-strange pentaquark could be its photoproduction on the nucleon. The chiral soliton model predicts that photoexcitation of the non-strange pentaquark has to be suppressed on the proton and should occur mainly on the neutron [7]. The mass of the non-strange pentaquark is expected to be near 1.7 GeV [5,8,9], with a total width of about 10 MeV and a partial width for the πN decay mode, less than 0.5 MeV [9].

Among various reactions, η photoproduction off the neutron is particularly attractive because (i) it selects only isospin $I = 1/2$ final states; (ii) there is enough accurate data for the “mirror” $\gamma p \rightarrow \eta p$ reaction; (iii) this reaction was considered as particularly sensitive to the signal of the non-strange pentaquark [5,7–9]. Up to now η photoproduction off the neutron

* Corresponding author at: Institute for Nuclear Research, 117312 Moscow, Russia.

E-mail addresses: slava@cpc.inr.ac.ru, slavak@jlab.org (V. Kuznetsov).

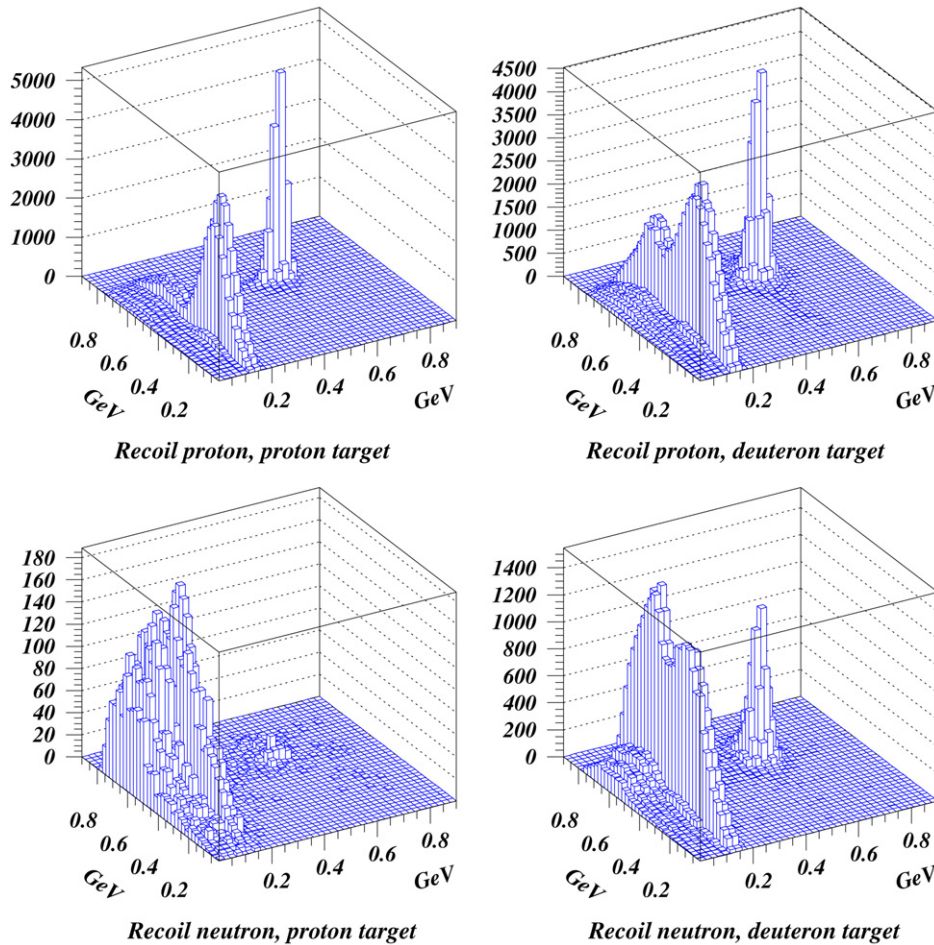


Fig. 1. Bi-dimensional spectra of invariant mass of two photons (X axis) versus missing mass $MM(\gamma N, N)$ calculated from momenta of recoil nucleons and the incoming photon (Y axis) for proton and deuteron targets.

has been explored mostly in the region of the $S_{11}(1535)$ resonance from threshold up to $W \sim 1.6$ GeV [10]. The ratio of cross sections, $(\gamma n \rightarrow \eta n)/(\gamma p \rightarrow \eta p)$, was found to be nearly constant, with a value near ~ 0.67 . At higher energies, the GRAAL Collaboration has reported a sharp rise of this ratio [11].

In this Letter we present the analysis of data collected at the GRAAL facility [12] in 2002. Both quasi-free $\gamma n \rightarrow \eta n$ and $\gamma p \rightarrow \eta p$ reactions were explored simultaneously, in the same experimental run, under the same conditions and solid angle using a deuteron target. Two photons from $\eta \rightarrow 2\gamma$ were detected in the BGO ball [13]. The η -mesons were identified by means of their invariant mass, with momentum reconstructed from the measured photon energies and angles. Recoil nucleons (neutrons or protons) were detected in two sets of detectors:

(i) Neutrons and protons emitted at forward angles $\theta_{\text{lab}} \leq 23^\circ$, passed through two planar multiwire chambers, a time-of-flight (TOF) hodoscope made of thin scintillator strips, and a lead-scintillator sandwich TOF wall [14]. The latter detector provides the detection of neutrons with an angular resolution of $2\text{--}3^\circ$ (full width at a half of maximum), and a TOF resolution of $600\text{--}800$ ps (FWHM). TOF measurement makes it possible to discriminate neutrons from photons and to reconstruct neutron momenta;

(ii) Recoil nucleons emitted at central angles $\theta_{\text{lab}} \geq 26^\circ$, were detected in the BGO ball [13]. This detector provides partial discrimination of neutrons from photons and no TOF measurement. The neutron energy was obtained using kinematics constraints.

Fig. 1 shows bi-dimensional plots of the $\gamma\gamma$ invariant mass versus the missing mass $MM(\gamma N, N)$ calculated from the momentum of the recoil nucleon (proton or neutron) and the momentum of the incoming photon. The plots have been obtained using data collected in experimental runs with proton and deuteron targets. A peak with coordinates ($X = m_\eta$, $Y = m_\eta$) corresponds to ηN photoproduction. A good ηp signal was obtained with the proton target, while only a few ηn events appeared in this run. Signals of both final states are clearly seen with the deuteron target.

As a first step of the analysis, the identification of the ηn and ηp final states was achieved in a way similar to that used in the previous measurements [16] on the free proton. The measured parameters of the recoil nucleon were compared with ones expected assuming a quasi-free reaction in which the photon interacts with only one nucleon bound in the deuteron while the second nucleon acts as a spectator.

At photon energies above 950 MeV, the background from $\gamma N \rightarrow \eta X N$ was observed. This background was clearly seen

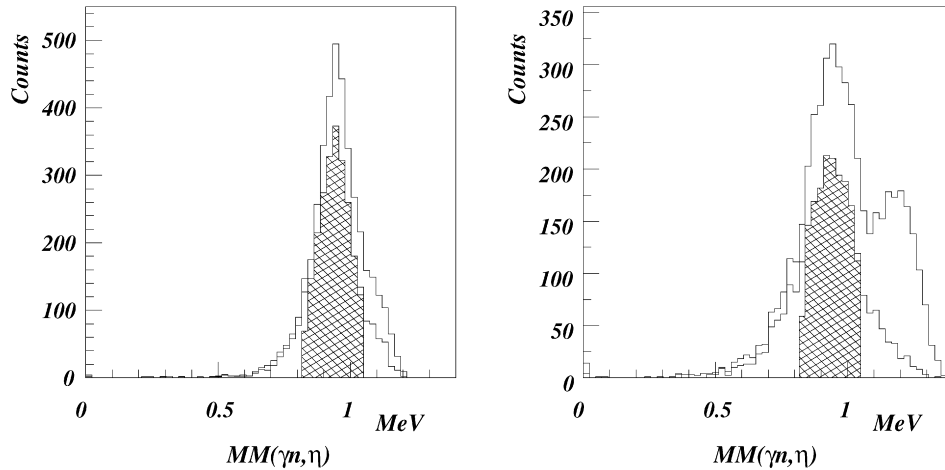


Fig. 2. Spectra of $MM(\gamma n, \eta)$ missing mass at photon energies $0.95 \leq E_\gamma \leq 1.2$ MeV (left panel) and $1.2 \leq E_\gamma \leq 1.5$ MeV (right panel). Upper curves correspond to initial selection. Lower curves indicate events after the cuts except the cut on $MM(\gamma n, \eta)$. Dashed areas show finally selected events.

in the spectrum of the $MM(\gamma N, \eta)$ missing mass in which it appeared as the second bump shifted to higher mass region from the position of the main peak at 0.94 GeV (Fig. 2). To reject this background, the cut on $MM(\gamma N, \eta)$ was imposed. In case of the neutron detection in the BGO ball, this cut was added by lower and upper limits on the BGO signal attributed to a neutron hit $0.014 \text{ GeV} \leq \Delta E \leq 0.5 * T_n$. The latter cut was found efficient to discriminate between neutrons and accidental low-energy photons emitted as secondary particles in the detector volume, and high-energy photons produced in background reactions.

In the case of a photon interaction with a nucleon bound in the deuteron, event kinematics is “peaked” around that on a free nucleon. Fermi motion of the target nucleon changes the effective energy of photon–nucleon interaction and affects momenta of outgoing particles. It also complicates discrimination of the background. Some events may suffer from rescattering and final-state interaction [18]. Such events might generate an artificial structure in the cross section due to specific effects like virtual subthreshold meson production followed by an interaction with the spectator nucleon [20].

The goal of the second stage of the analysis was to minimize any influence of rescattering, final-state interaction, or background contamination. Here, we used the sample of events in which the recoil neutrons/protons were detected in the forward detectors. The strategy at this stage was to study the dependence of the spectra of selected events on cuts. The recoil nucleon missing mass $MM(\gamma N, \eta)$, $TOF_{\text{meas}} - TOF_{\text{exp}}$, and $\theta_{\text{meas}} - \theta_{\text{exp}}$ selection windows were reduced by a factor 2–3. Tight cuts preferably reject rescattering, final-state interaction, and the remaining background. They also suppress those events whose kinematics is strongly distorted by Fermi motion or in which one or more parameters of the outgoing particles are not properly measured, due to detector response.

Four types of spectra were considered at this stage:

(i) The spectrum of the center-of-mass energy W calculated from the momentum of the initial-state photon and assuming the target nucleon to be at rest $W = \sqrt{(E_\gamma + M_N)^2 - E_\gamma^2}$. This

quantity ignores Fermi motion and is peaked around the effective center-of-mass energy (40–60 MeV (FWHM) depending on the energy of the incoming photon).

(ii) The spectrum of the center-of-mass energy reconstructed as the invariant mass of the final-state η and the nucleon $M(\eta N)$. This quantity is much less smeared by Fermi motion (about 2 MeV (FWHM)) but includes large uncertainties due to instrumental resolution (40–60 MeV (FWHM)).

(iii) Distribution of the momentum for the spectator nucleon, reconstructed as the “missing” momentum from the momenta of the final-state η and nucleon and the momentum of the incoming photon;

(iv) Difference between the final-state $M(\eta N)$ invariant mass and the initial-state center-of-mass energy W .

The upper row of Fig. 3 shows the $M(\eta n)$ (first column) and W (second column) spectra obtained with the initial cuts. Both exhibit a shoulder-like bump in the region of 1.6–1.7 GeV on the slope of the $S_{11}(1535)$ resonance. The spectator-momentum (third column) and the $M(\eta n) - W$ distributions (fourth column) are relatively broad. Plots in the middle row correspond to the tight cuts. Here the spectator-momentum spectrum is more compressed. The $M(\eta n) - W$ spectrum is more narrow and is localized near 0. The bumps observed in the previous $M(\eta n)$ and W spectra, become more pronounced and are transformed into peaks near 1.68 GeV. Conversely, events rejected by the second-level cuts (lower row) form a broader spectator-momentum distribution with the maximum near 0.1 GeV/c. The $M(\eta n) - W$ difference contains two maxima, both shifted from 0. The $M(\eta n)$ and W spectra show some hints on lateral peaks.

The same procedure was applied to the quasi-free $\gamma p \rightarrow \eta p$ reaction (Fig. 4). The spectator momentum and $M(\eta p) - W$ spectra are similar to those obtained on the neutron. However, the $M(\eta N)$ and W spectra are smooth and exhibit no structure.

Evolution of spectra in Figs. 3, 4 suggests that most of events rejected by the second-level cuts either strongly suffer from Fermi motion and/or detector response, or possibly originate from rescattering and final-state interaction. However, events shown in the middle-row plots, correspond to quasi-free re-

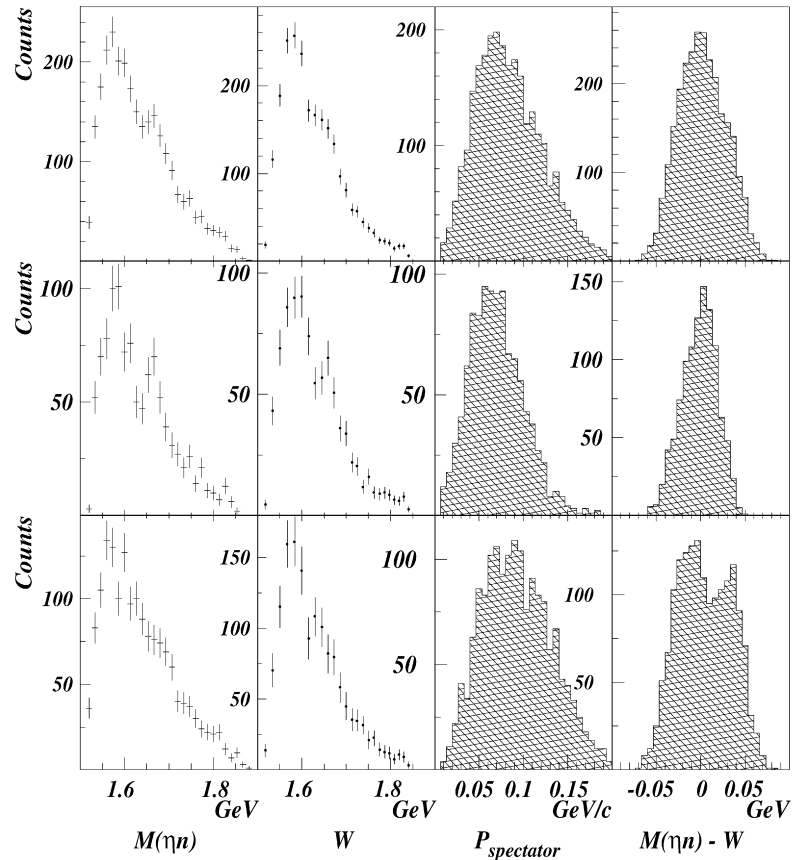


Fig. 3. $\gamma n \rightarrow \eta n$ data. Spectra of center-of-mass energy, calculated as invariant mass of final-state η and the nucleon (left columns), from the energy of the incoming photon and assuming the target nucleon to be at rest (second columns), momentum of the spectator nucleon (third columns), and difference between final-state and initial-state center-of-mass energies (fourth columns). Upper rows correspond to initial selection, middle rows show spectra after tight cuts, lower rows show events rejected by tight cuts.

actions. These spectra clearly reveal a peak at 1.68 GeV in η photoproduction on the neutron which is not seen on the proton.

The measured quasi-free differential cross sections for ηn and ηp photoproduction are shown in Fig. 5. The common normalization for both protons and neutrons was done by comparing quasi-free proton data at backward angles with the E429 solution of the SAID $\gamma p \rightarrow \eta p$ partial-wave analysis [21] and η -MAID prediction [17] for η photoproduction on the free proton, which were folded with Fermi motion (upper row, right panel of Fig. 5). The measured spectra of events were corrected on the simulated detection efficiency and on the beam spectrum. In addition the spectra of $\gamma n \rightarrow \eta n$ events were corrected on the difference between the measured and simulated efficiencies of the neutron detection. The neutron detection efficiency was determined using the previous data for the $\gamma p \rightarrow \pi^+ n$ reaction [15]. It was found to be about 22% for the shower wall and 27% for the BGO ball being dependent the neutron energy, on the pulse height thresholds set for both detectors, and on cuts used to identify neutrons. The obtained distributions were then scaled by a common constant factor. The latter was determined requesting the minimum of the difference between quasi-free proton data at backward angles and the SAID and MAID solutions. The region of backward angles was chosen for the normalization because of the coincidence in shapes

of the cross section on the proton and the SAID and MAID solutions (top right panel of Fig. 5). This coincidence hints a small role of nuclear effects at these angles. At more forward angles, rescattering and final-state interaction seem to become more significant reaching $\sim 30\%$ in the region of the $S_{11}(1535)$ resonance. Error bars shown in Fig. 5 correspond to statistical uncertainties only. The normalization uncertainty of 10% originates mostly from the quality of simulations of quasi-free processes and from uncertainties in determining the neutron detection efficiency.

The cross section on the neutron clearly reveals a bump-like structure¹ near $W \sim 1.68$ GeV. This structure looks slightly wider at forward angles. The visible width of the peak at forward angles is about 80–100 MeV (FWHM) (or $rms = 35$ –40 MeV). The data have been compared with an isobar model for η photo- and electroproduction η -MAID [17]. The model includes 8 main resonances and suggests the dominance of the $S_{11}(1535)$ and $D_{15}(1675)$ resonances in η photoproduction off the neutron below $W \sim 1.75$ GeV. The model predicts a bump-like structure near $W \sim 1.7$ GeV in the total η photo-

¹ The cross-section obtained with tight cuts exhibit a slightly more narrow structure but includes larger statistical and systematic errors. For the sake of clarity and reliability in our conclusions it is not shown.

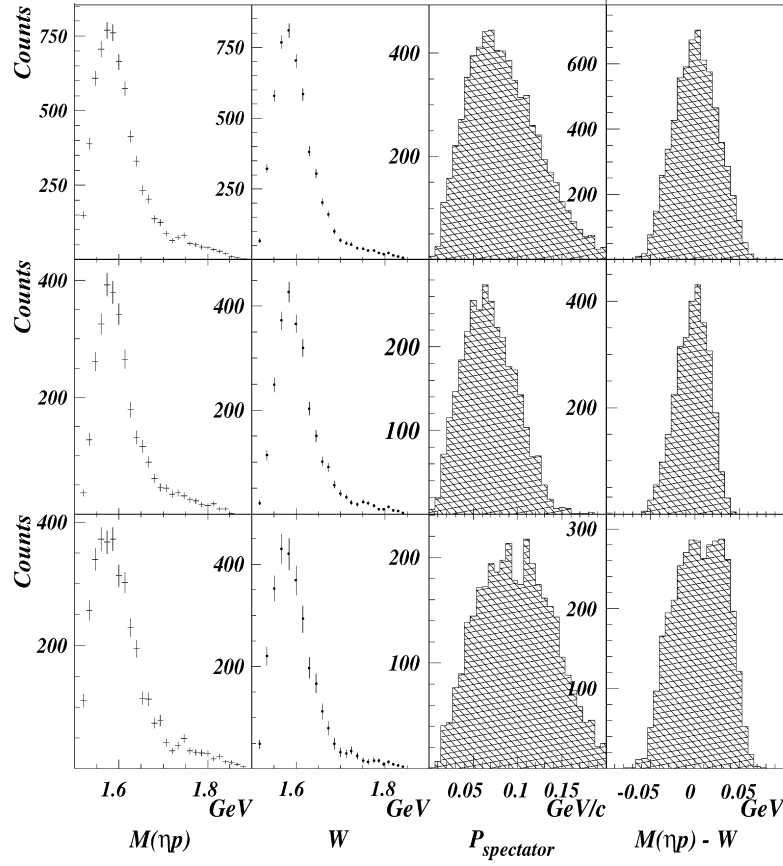


Fig. 4. $\gamma p \rightarrow \eta p$ data. The legend is the same as for Fig. 3.

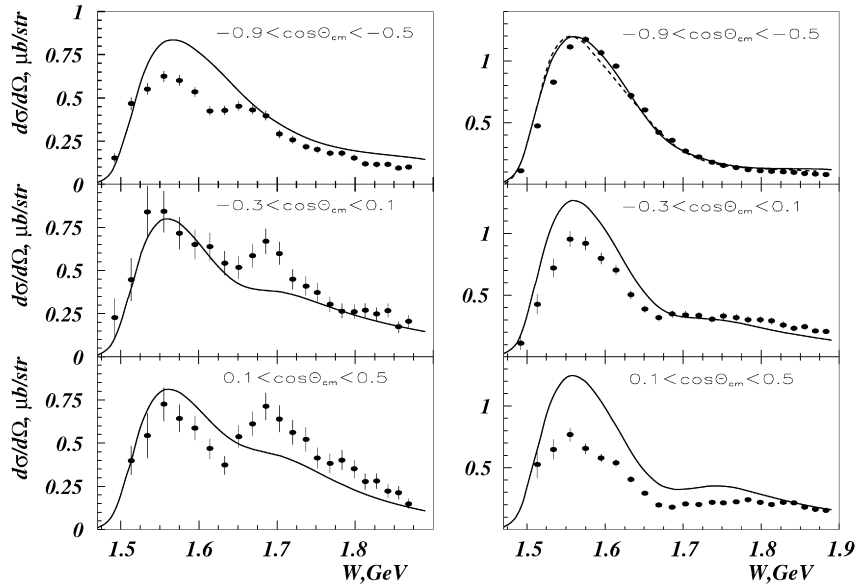


Fig. 5. Quasi-free differential cross section at different angles. Left panel: $\gamma n \rightarrow \eta n$. Right panel: $\gamma p \rightarrow \eta p$. Solid lines are η -MAID predictions for η photo-production on the free neutron/proton folded with Fermi motion. Dashed line is E429 solution of the SAID $\gamma p \rightarrow \eta p$ partial wave analysis folded with Fermi motion.

production cross section on the neutron [23]. This structure is caused by the $D_{15}(1675)$ resonance. The η -MAID differential cross sections are smooth (Fig. 5, left panel). The PDG estimate for the $D_{15}(1675)$ ηN branching ratio $\Gamma_{\eta N}/\Gamma_{\text{total}}$ is close

to 0 while the value included into η -MAID is 17% [23]. The PDG average for the Breit–Wigner width of this resonance is $\Gamma \sim 150$ MeV [1]. The structure observed in the quasi-free cross section looks more narrow.

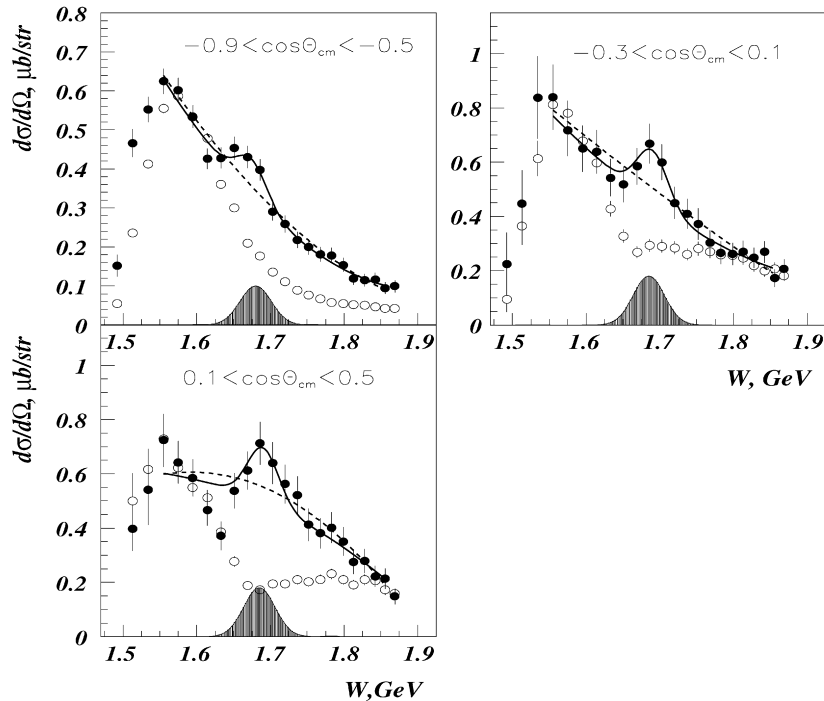


Fig. 6. Polynomial-plus-narrow-state fit of $\gamma n \rightarrow \eta n$ cross sections. Black circles are $\gamma n \rightarrow \eta n$ data. Open circles correspond to $\gamma p \rightarrow \eta p$ cross section normalized on the cross section on the neutron in the maximum of the $S_{11}(1535)$ resonance. Dashed areas show simulated contribution of the narrow state. Solid lines are the result of the fit. Dashed lines show the fit by 3-order polynomial only.

It is well known that η photoproduction on the proton is dominated by photoexcitation of the $S_{11}(1535)$ resonance up to $W \sim 1.68$ GeV. At higher energies, the increasing role of higher-lying resonances is expected [16,19]. η photoproduction on the neutron is dominated by the $S_{11}(1535)$ up to $W \sim 1.62$ GeV [10,11]. The shape of cross sections on the neutron and on the proton in the region $S_{11}(1535)$ resonance below $W \sim 1.62$ GeV is similar (Fig. 6). One may assume that the enhancement in the cross section on the neutron at $W \sim 1.62$ – 1.72 GeV is caused by an additional relatively narrow resonance. In Fig. 6 the simulated contribution of a narrow state ($M \sim 1.68$ GeV, $\Gamma = 10$ MeV) is shown. This state appears as a wider bump in the quasi-free cross section due to Fermi motion of the target neutron. The neutron cross section in the range of $W \sim 1.55$ – 1.85 GeV is well fit by the sum of a third-order polynomial and a narrow state, with an overall χ^2 about 11/14, 8/14 and 11/14 for the backward, central and forward angles respectively. The fit by only a third-order polynomial increases χ^2 to about 31/15, 21/15, and 23/15.

Thus, the apparent width of the structure in the $\gamma n \rightarrow \eta n$ cross section is not far from one expected due to smearing by Fermi motion. The same structure was observed in the $M(\eta n)$ invariant mass spectra (Fig. 3). The width of the peaks in the $M(\eta n)$ spectra is also close to experimental resolution. Therefore this structure may signal the existence of a relatively narrow ($\Gamma \leq 30$ MeV) state. If so, its properties, the possibly narrow width and the strong photocoupling to the neutron, are certainly unusual. There are six well-known nucleon resonances in this mass region [1]: $S_{11}(1650)$, $D_{15}(1675)$, $F_{15}(1680)$, $D_{13}(1700)$, $P_{11}(1710)$, and $P_{13}(1720)$. Among them $D_{15}(1675)$ was predicted to have stronger pho-

tocouplings to the neutron [2,3]. One cannot exclude that the observed structure might be a manifestation of one of them or might originate from the interference between several resonances. On the other hand, such a state coincides with the expectation of the chiral soliton model [7,8] and a modified PWA [9] for the non-strange pentaquark.²

The possible role of some resonances has been recently examined in Refs. [23–25] on the base of our [26] and CB-TAPS [27] preliminary reports. In the standard η -MAID model the $D_{15}(1675)$ resonance produces a bump near $W \sim 1.68$ GeV in the total η -photoproduction cross section on the neutron. The unusually large branching ratio of $D_{15}(1675)$ to ηN is needed to reproduce experimental data. The inclusion of a narrow $P_{11}(1675)$ resonance with parameters suggested in [7] into η -MAID generates a narrow peak in the cross section on the free neutron while the cross section on the free proton remains almost unaffected. The peak is transformed into a wider bump similar to experimental observation if Fermi motion is taken into account [23]. The similar result has been obtained in Ref. [24]. Authors of [25] have demonstrated that the peak at $W \sim 1.67$ GeV in the η -photoproduction cross section on the neutron can be explained in terms of the $S_{11}(1650)$ and $P_{11}(1710)$ resonance excitation.

The decisive identification of the observed structure requires a complete partial-wave analysis based on a fit to experimental data. New beam asymmetry data from GRAAL and cross

² Here we note that the recent negative reports on the search for the $\Theta(1540)$ pentaquark [22] put doubts on the existence of the exotic antidecuplet and the non-strange pentaquark.

sections from the CB/TAPS Collaboration [27] and from Laboratory of Nuclear Sciences of Tohoku University [28] are expected to enlarge the data base. The problem is that such analysis requires a fit to quasi-free data smeared by Fermi motion and distorted by rescattering and final-state interaction. The use of the beam asymmetry Σ is going to be even more sophisticated: considerable theoretical effort is needed to understand the interaction of polarized photons with bound nucleons [29]. More perspective seems to search for the traces of this state in reactions on the free proton. Another way is to study the $\gamma n \rightarrow \eta n$ reaction in experiments with the detection of the spectator proton, and/or in double-polarization experiments with parallel/antiparallel beam–target polarisations. A spin-1/2 state would be seen only with antiparallel (helicity-1/2) beam–target polarisations. Such dedicated experiments could be carried out at JLAB and the upgraded ELSA and MamiC facilities.

Acknowledgements

It is a pleasure to thank the staff of the European Synchrotron Radiation Facility (Grenoble, France) for stable beam operation during the experimental run. We thank Y. Azimov, K. Goeke, and M. Polyakov for the valuable theoretical contribution in support of this work, R. Workman and I. Strakovsky for the assistance in preparation of a manuscript. Discussions with W. Briscoe, V. Burkert, D. Diakonov, A. Dolgolenko, I. Jaegle, H.-C. Kim, M. Kotulla, B. Krusche, A. Kudryavtsev, V. Mokeev, E. Pasyuk, P. Pobylitsa, M. Ripani, A. Sibirtsev, I. Strakovsky, M. Tauti, L. Tiator and R. Workman were very helpful. This work has been supported by Università degli studi di Catania and Laboratori Nazionale del Zud, INFN Sezione di Catania (Italy), and by Ruhr-Universität Bochum (Germany).

References

- [1] S. Eidelman, et al., Phys. Lett. B 592 (2004) 1.
- [2] A.J.G. Hey, J. Weyers, Phys. Lett. B 48 (1974) 69.
- [3] V. Burkert, et al., Phys. Rev. C 67 (2003) 035205.
- [4] D. Diakonov, V. Petrov, M. Polyakov, Z. Phys. A 359 (1997) 305.
- [5] R. Jaffe, F. Wilczek, Phys. Rev. Lett. 91 (2003) 232003, hep-ph/0307341.
- [6] V. Burkert, hep-ex/0510309, and references therein.
- [7] M. Polyakov, A. Rathke, Eur. Phys. J. A 18 (2003) 691, hep-ph/0303138; H.C. Kim, et al., Phys. Rev. D 71 (2005) 094023, hep-ph/0503237.
- [8] D. Diakonov, V. Petrov, Phys. Rev. D 69 (2004) 094011, hep-ph/0310212.
- [9] R. Arndt, et al., Phys. Rev. C 69 (2004) 035208, nucl-th/0312126.
- [10] B. Krusche, et al., Phys. Lett. B 358 (1995) 40; V. Heiny, et al., Eur. Phys. J. A 6 (2000) 83; J. Weiß, et al., Eur. Phys. J. A 16 (2003) 275, nucl-ex/0210003; P. Hoffman-Rothe, et al., Phys. Rev. Lett. 78 (1997) 4697.
- [11] V. Kouznetsov, et al., in: E. Swanson (Ed.), Proceedings of Workshop on the Physics of Excited Nucleons NSTAR2002, Pittsburgh, USA, 9–12 October 2002, World Scientific, 2003, pp. 267–270.
- [12] General description of the GRAAL facility is in V. Bellini, et al., Eur. J. A 26 (2006) 299.
- [13] F. Ghio, et al., Nucl. Instrum. Methods A 404 (1998) 71.
- [14] V. Kouznetsov, et al., Nucl. Instrum. Methods A 487 (2002) 128.
- [15] O. Bartalini, Phys. Lett. B 544 (2002) 113, hep-ex/0207010.
- [16] J. Ajaka, et al., Phys. Rev. Lett. 81 (1998) 1787; F. Renard, et al., Phys. Lett. B 528 (2002) 215.
- [17] W.-T. Chiang, S.-N. Yang, L. Tiator, D. Drechsel, Nucl. Phys. A 700 (2002) 426, hep-0110034, <http://www.kph.uni-mainz.de>.
- [18] A. Baru, A. Kudryavtsev, V. Tarasov, Phys. At. Nucl. 67 (2004) 743, nucl-th/0301021; A. Sibirtsev, S. Schneider, C. Elster, Phys. Rev. C 65 (2002) 067002, nucl-th/0203039; A. Fix, H. Arenhovel, Phys. Rev. C 68 (2003) 44002, nucl-th/0203039, and references therein.
- [19] M. Dugger, et al., Phys. Rev. Lett. 89 (2002) 222002; V. Crede, et al., Phys. Rev. Lett. 94 (2004) 012004, hep-ex/0311045.
- [20] Y. Iieva, et al., Nucl. Phys. A 737 (2004) S158, nucl-ex/0309017.
- [21] R.A. Arndt, W.J. Briscoe, I.I. Strakovsky, R.L. Workman, <http://gwdac.phys.gwu.edu>, in preparation.
- [22] M. Battaglieri, et al., CLAS Collaboration Phys. Rev. Lett. 96 (2006) 042001, hep-ex/0510061; C. Niccolai, et al., CLAS Collaboration, Phys. Rev. Lett. 97 (2006) 032001, hep-ex/0604047.
- [23] L. Tiator, Talk at Work on η -nucleus physics, Jülich, Germany, 8–12 May 2006, nucl-th/0610114.
- [24] K.-S. Choi, S. Nam, A. Hosaka, H.-C. Kim, Phys. Lett. B 636 (2006) 253, hep-ph/0512136.
- [25] V. Shklyar, A. Leshke, U. Mozel, nucl-th/0611036.
- [26] V. Kuznetsov, et al., in: Proceedings of Workshop on the Physics of Excited NSTAR2004, Grenoble, March 2004, World Scientific, 2004, p. 197, hep-ex/0409032; V. Kuznetsov, et al., in: Proceedings of Nucleons NSTAR2005, Tallahassee, FL, USA, October 2005, World Scientific, 2006, hep-ex/0601002.
- [27] J. Jaegle, Talk at Workshop on the Physics of Excited Nucleons NSTAR2005, Tallahassee, FL, USA, 12–15 October 2005.
- [28] J. Kasagi, Talk at Yukawa International Seminar YKIS2006, 20 November–December 2006, Kyoto, Japan, <http://www2.yukawa.kyoto-u.ac.jp/ykis06/>.
- [29] A. Sibirtsev, Talk at Workshop on eta photoproduction, Bochum, Germany, 12–15 February 2006.